Calculation of river sediment fluxes from uncertain and infrequent measurements

B. Cheviron, Magalie Delmas, Olivier Cerdan, J.M. Mouchel

Author-produced version of the article published in Journal of Hydrology, 2014, N°508, p. 364-373
The original publication is available at http://www.sciencedirect.com
Doi: 10.1016/j.jhydrol.2013.10.057

Calculation of river sediment fluxes from uncertain and infrequent measurements

Bruno Cheviron[1,*], Magalie Delmas[2], Olivier Cerdan[3] & Jean-Marie Mouchel[4]

1: UMR G-EAU, IRSTEA, 361 rue Jean-François Breton, 34196 Montpellier Cedex 05, France - bruno.cheviron@irstea.fr

2: UMR LISAH, INRA, 2 place Pierre Viala, 34060 Montpellier Cedex 01, France - magalie.delmas@supagro.inra.fr

3: BRGM, 3 avenue Claude Guillemin, BP6009, 45060 Orléans Cedex 2, France - o.cerdan@brgm.fr

4: UMR SISYPHE, Université Paris VI-Pierre et Marie Curie, 4 place Jussieu, 75252 Paris Cedex 05, France - jean-marie.mouchel@upmc.fr

* corresponding author, tel: +33 (00) 4 67 04 63 64

Keywords: River flow, sediment transport, uncertainty analysis, rating curves.

Author-produced version of the article published in Journal of Hydrology, 2014, N°508, p. 364-373
The original publication is available at http://www.sciencedirect.com
Doi: 10.1016/j.jhydrol.2013.10.057

Abstract

This paper addresses feasibility issues in the calculation of fluxes of suspended particulate matter (SPM) from degraded-quality data for flow discharge (Q) and sediment concentration (C) under the additional constraints of infrequent and irregular sediment concentration samplings. A crucial setting of the scope involves establishing the number of data required to counterbalance limitations in the measurement accuracy and frequency of data collection. This study also compares the merits and drawbacks of the classical rating curve ($C=aQ^b$) with those of an improved rating curve approach (IRCA: $C=aQ^b+a_1\delta S$) in which the correction term is an indicator of the variations in sediment storage, thus relating it to flow dynamics. This alternative formulation remedies the known systematic underestimations in the classical rating curve and correctly resists the degradation in data quality and availability, as shown in a series of problematic though realistic cases. For example, monthly concentration samplings (in average) with a random relative error in the [-30%, +30%] range combined with daily discharge records with a systematic relative error in the [-5%, +5%] range still yield SPM fluxes within factors of 0.60-1.65 of the real value, provided that 15 years of data are available. A shorter 5-day time interval (on average) between samplings lowers the relative error in the SPM fluxes to below 10%, a result directly related to the increased number of Q-C pairs available for fitting. For regional-scale applications, this study may be used to define the data quality level (uncertainty, frequency and/or number) compatible with reliable computation of river sediment fluxes. Provided that at least 200 concentration samplings are available, the use of a sediment rating curve model augmented to account for storage effects fulfils this purpose with satisfactory accuracy under real-life conditions.

Author-produced version of the article published in Journal of Hydrology, 2014, N°508, p. 364-373
The original publication is available at http://www.sciencedirect.com
Doi: 10.1016/j.jhydrol.2013.10.057

1. Introduction

Sediment fluxes in fluvial systems reflect the denudation processes that occur on the earth's surface and exert a controlling effect on the fates of nutrients, organic pollutants and heavy metals. Therefore, assessment of sediment fluxes aids in characterising the impact of particulate transfer on water quality throughout the river system. However, the estimation of realistic sediment budgets requires long-term discharge-concentration data (Walling and Webb 1985, Ludwig and Probst 1998, Webb et al. 2003, Delmas et al. 2009), which often suffer from poor availability and reliability (Meybeck et al. 2003, Walling and Fang 2003). In particular, uncertainties in both the sampling and calculation methods affect the measurement of sediment concentration (SPM) fluxes (Rode and Surh 2007). Moreover, significant drifts in the measured quantities may arise due to the location of the sampling in the river section because the suspended sediment concentration varies within cross-sections of the rivers, thus necessitating a series of depth- and width-integrated measurements (Horowitz, 1997). However, in most cases, modellers and decision-makers use the daily discharge records combined with infrequent sediment concentration samplings, which are generally collected at a single location and exhibit high temporal variability.

Previous studies have indicated how increased sampling frequencies and total periods of data collection can reduce uncertainties in the predicted SPM or trace element fluxes (Horowitz et al. 2001, Coynel et al. 2004, Moatar and Meybeck 2005, Rode and Surh, 2007), but a complementary and perhaps broader strategy would involve treatment of the analysis in terms of the interactions between the number of data, the time interval between samplings (affected by a realistic random component) and the total period of the data collection. This analysis would be particularly pertinent in the numerous areas where available the sediment concentration data are by-products of programs for water quality monitoring that involve infrequent (approximately monthly) sampling (Delmas et al. 2012). A relevant and widely used methodology is the reconstruction of continuous (daily)

Author-produced version of the article published in Journal of Hydrology, 2014, N°508, p. 364-373
The original publication is available at http://www.sciencedirect.com
Doi: 10.1016/j.jhydrol.2013.10.057

fluctuations in the sediment concentration from the empirical relationships ($C(Q)$ rating curves) that link the sediment concentration (C) to the water discharge (Q) values. The classical $C(Q)=aQ^b$ rating curve is often used for this purpose. Nevertheless, for sediment transport studies, the occasional strong non-linearity in the $C(Q)$ relationship and the presence of only a few extreme events point to well known and problematic cases when fitting power laws (Laherrere 1996, Goldstein et al. 2004). These problematic cases suggest the use of truncated intervals of Q values (Moatar et al. 2012) or data subdivision and hypothesising of the distinct $C(Q)$ relationships with the seasons, basin sizes or properties (Walling and Webb 1981, Smart et al. 1999, Quilbé et al. 2006; Delmas et al. 2009). Another possibility is the addition of correction terms (Laherrere and Sornette 1998) with a user-defined physical meaning. Ferguson (1986, 1987) chose the latter option in his inaugural papers that tackled the advantages and limitations in estimating sediment fluxes from power-law rating curves. Similar to other research domains, an open question is whether to attribute a deterministic physical meaning to the pre-factor and the exponent (Peters-Kümmerly 1973, Morgan 1995, Asselmann 2000) or to consider them as conceptually imperfect though demonstrably statistically relevant. Addressing these questions with a clear physical sense opens the door for a wide series of improved rating curves and variants, as advocated by Phillips et al. (1999), Asselmann (2000), Horowitz (2003) and Delmas et al. (2011), among others. For example, Picouet et al. (2001) hypothesised two sediment sources (bank and hillslope erosion), and Mano et al. (2009) introduced explicit climatic and topographic factors.

The objective of the current paper is to address the precision and sensitivity issues that exist in prediction of SPM fluxes for typical cases with data of degraded-quality gathered from infrequent samplings. We consider the C and Q measurements to be affected by errors of different types and magnitudes. As commonly reported, we hypothesised a higher probability of error for concentration than for discharge measurements. Concentration data were considered prone to random errors in a [-30%, +30%] interval around the measured values, whereas five systematic biases were tested for

Author-produced version of the article published in Journal of Hydrology, 2014, N°508, p. 364-373
The original publication is available at http://www.sciencedirect.com
Doi: 10.1016/j.jhydrol.2013.10.057

discharge data in the [-20%, 20%] interval around the daily records. Moreover, infrequent concentration measurements were simulated together with slightly perturbed sampling periods. The framework of this study compares the merits and drawbacks of the classical rating curve with those of an improved rating curve approach. The latter includes a correction term as an indicator of sediment storage, thus relating the variation to flow dynamics. This work relies on a USGS dataset encompassing multiple rivers, basin typologies and years.

2. Material & Methods

2.1 Database

The present study relies on daily discharge-concentration data collected over several years at 22 USGS stations taken from the larger dataset available at http://waterdata.usgs.gov/. The selected stations cover a wide range of river basin typologies and sizes and are associated with specific discharge and SPM statistics (Table 1). For the Des Moines River station, we chose to split the records into two distinct periods because we observed notably large discharge variations over the first years of data collection (1961-1977) followed by rather limited variation over the most recent years (1977-2004). Several stations display notably low water levels and even close to intermittent flows under severe winter conditions (e.g., station 21, Salinas River near Spreckels), summer droughts (e.g., station 18, Kaskaskia River at Cook Mills) or both (e.g., station 7, Hocking River at Athens). However, stations in the USGS database that exhibit complete drying or glaciations have been discarded from the analysis because they require different treatment. This choice tends to omit basins with small drainage areas, especially those that experience sharp climatic conditions. Nevertheless, various temperate to continental climates are accounted for at stations in California (CA), Illinois (IL), Iowa (IA), Missouri (MI), North Carolina (NC), Ohio (OH) and Virginia (VA). Another merit of sufficiently large basins for the present study is response times that are greater than the reference daily

Author-produced version of the article published in Journal of Hydrology, 2014, N°508, p. 364-373
The original publication is available at http://www.sciencedirect.com
Doi: 10.1016/j.jhydrol.2013.10.057

sampling period for the discharge and concentration measurements. In addition to the temporal arguments, large basins are also more integrative than smaller basins because they offer additional spatial variability with respect to the sediment sources and delivery processes combined with larger climatic variability.

[TABLE 1 ABOUT HERE]

2.2 Rating curves

In addition to the classical $C=aQ^b$ rating curve (RC), different expressions and strategies have been tested and described in detail by Delmas et al. (2011). Among these, emphasis is placed in this work on the Improved Rating Curve Approach (IRCA), which hypothesises $C=aQ^b+a_1\delta S$, where a_1 is a parameter, S is the sediment storage index and δS is the daily variation. This method operates in two steps. First, the method fits the $C=aQ^b$ model, thus freezing the a and b coefficients, and subsequently fits the a_1 parameter, which is the only remaining degree of freedom in the $a_1\delta S$ correction term. The IRCA was implemented to remedy the known limitations of the RC, especially its inability to include flow dynamics or antecedent flow conditions in the prediction of C values.

For this purpose, the sediment storage index is described as a function of discharge dynamics:

$$S(t) = \exp\left(-A\frac{q(t)}{Q_0}\right) \quad [1]$$

where A is a dimensionless coefficient that controls the amplitude of S variations, and $q(t)$ is the instantaneous $Q(t)$ value on the rising limbs of the hydrograph or a sliding average of $Q(t)$ values on the falling limbs. This double status of $q(t)$ ensures asymmetry between quick sediment loading and delayed sediment storage, which is the working hypothesis that underlies the IRCA. The sliding average extends itself backwards in time towards the beginning of the current falling limb but is

Author-produced version of the article published in Journal of Hydrology, 2014, N°508, p. 364-373
The original publication is available at http://www.sciencedirect.com
Doi: 10.1016/j.jhydrol.2013.10.057

limited to 20 days at most, which is the chosen approach used to account for antecedent flow conditions.

The IRCA also requires statistical analysis to establish the upper limit of the base flow, given as Q_0. From the adopted assumptions, S varies between 0 for extreme discharges (all possible sediments present in the flow) and 1 when flow ceases (all material stored and available). The choice of A=0.1 yields S=0.95, 0.75, 0.50, 0.25 and 0.05 for q/Q_0 ratios of approximately 0.5, 3, 7, 14 and 30, respectively. This choice also implies that $S\approx0.9$ for $q=Q_0$, and thus the "sediment availability" would be approximately 90%.

Figure 1 shows the variations in the sediment storage index in an application to the Hocking River at Athens (station 7, Table 1). The figure displays the main characteristics of this approach: asymmetry between the delayed sediment storage and quick sediment mobilisation, damping of the high-frequency oscillations and maximum sediment storage associated with long-lasting low discharges. The intent of the IRCA is to use the daily variations of the sediment storage index as relevant information for the flow dynamics, as handled by the $a_1\delta S$ correction term in the $C=aQ^b+a_1\delta S$ model.

[FIGURE 1 ABOUT HERE]

In a strict sense, both the $C=aQ^b+a_1\delta S$ and $C=aQ^b+a_1\delta S$ expressions should be considered in this work as "models" and not "laws". Laws should be written with an additional explicit error term, either multiplicative or additive, whose distribution should be assessed from the characteristics and is missing in the data (Q, C) measurements. This option would take into account that the $C=aQ^b$ and $C=aQ^b+a_1\delta S$ expressions are exact formulations of the problem, attributing the deviations between the calculated and observed quantities to variations in the associated error terms. Instead, the current option views the $C=aQ^b$ and $C=aQ^b+a_1\delta S$ expressions as imperfect models with inherent

Author-produced version of the article published in Journal of Hydrology, 2014, N°508, p. 364-373
The original publication is available at http://www.sciencedirect.com
Doi: 10.1016/j.jhydrol.2013.10.057

errors. Therefore, the scope of this work focuses on the dispersion of the model predictions with alterations of the (Q, C) dataset.

2.3 Fitting procedures

All fittings were automated using a multi-stage procedure centred on the PEST parameter estimation software (Doherty, 2004) but also resorted to further programming. Figure 2 displays the simplified flow chart, which is briefly described. The user selects a $C(Q)$ model with p parameters to fit, entering the flow chart with the initial p_0 vector of parameter values and also providing a series of Q_i discharge samplings. This (Q_i, p) set is processed via a program that calculates the "fitted" $C_i^{(f)}$ value associated with each Q_i value for the selected power law. Next, PEST carries out an overall optimisation based on the minimisation of an objective function, which is calculated as the sum of the squared residuals between the observed C_i values and the fitted $C_i^{(f)}$ values. Once the optimisation has been completed, PEST estimates the goodness-of-fit by calculating the coefficient of determination, known as R. The R value may therefore be used for comparisons between fittings. One of the interesting features in PEST is its ability to handle power laws with or without log transformations, and the choice is left to the user's discretion. Slightly better results have been obtained in this work by fitting the untransformed expressions.

[FIGURE 2 ABOUT HERE]

2.4 Methods for calculating fluxes and errors

The real amount of exported sediment in the [0, T] total time period is the unknown SPM flux:

$$F = \int_0^T Q(t)C(t)dt \qquad [2]$$

where Q is the discharge, C is the concentration of suspended particulate matter (SPM) and t is time.

Author-produced version of the article published in Journal of Hydrology, 2014, N°508, p. 364-373
The original publication is available at http://www.sciencedirect.com
Doi: 10.1016/j.jhydrol.2013.10.057

191

192 The straightforward approximation for direct calculation of *F* is:

$$F_N = \sum_{i=1}^{N} Q_i C_i \delta t_i \quad [3]$$

193 where Q_i and C_i are time-averaged values over the δt_i intervals covering the [0, *T*] time period.

194

195 The discrepancy between *F* and F_N plausibly increases with increased δt_i values. Nevertheless, certain
196 rare and fortuitous combinations of large δt_i values may still lead to $F_N \approx F$, from compensating
197 effects between the underestimations and overestimations of SPM fluxes over certain periods.
198 Therefore, the gap between F_N and *F* is not expected to vary in any monotonous or linear manner
199 with increasing δt_i values. By contrast, the δt_i intervals that are smaller than the characteristic time
200 period of fluctuations in *Q* and *C* values tend to ensure the reliability of the F_N approximation.
201 Because the SPM regimes are related to the basin sizes (Meybeck et al. 2003) and only drainage
202 areas larger than 1000 km^2 are considered in this work, the F_N fluxes calculated from the error-free
203 daily discharge and concentration records are considered as exact solutions ($F_N \approx F$) in the following.
204 The subsequent developments aim to test the deviations from this best-case scenario that appear
205 when coping with infrequent and/or uncertain data (i.e., random errors in the concentration data
206 and systematic errors in the discharge data and sparse concentration samplings in this work).

207

208 The missing concentration data in [3] may be replaced by concentration values obtained from the
209 fitted *C*(*Q*) models. Each Q_i datum results in a predicted $C_i^{(f)}$ concentration value, and the exported
210 SPM flux now can be approximated by:

$$F_{N,f} = \sum_{i=1}^{N} Q_i C_i^{(f)} \delta t_i \quad [4]$$

211

Author-produced version of the article published in Journal of Hydrology, 2014, N°508, p. 364-373
The original publication is available at http://www.sciencedirect.com
Doi: 10.1016/j.jhydrol.2013.10.057

212 The hypothesis for the missing *C* data implies that only $n<N$ values have been measured. In the
213 calculation of $F_{N,f}$, one may either use the available concentration data C_i instead of the fitted values
214 or systematically resort to the entire series of $C_i^{(f)}$ values, as in this study.

215

216 From a theoretical point of view, any given $C_i^{(f)}$ is an unknown function of the entire dataset via the
217 fitting procedure:

$$C_i^{(f)} = C_i^{(f)}(Q_1, \ldots, Q_N, C_1, \ldots, C_n, \Delta t_1, \ldots, \Delta t_k, \ldots, \Delta t_n) \quad [5]$$

218 with irregular Δt_k intervals between successive *C* samplings in the general case.

219

220 For regular Δt intervals between concentration samplings, the $(\Delta t_1,\ldots,\Delta t_k,\ldots,\Delta t_n)$ temporal argument
221 could be reduced to (Δt, *n*) or (Δt, *T*) without any additional loss of information. Combining these
222 elements with shortened notations $Q'=(Q_1,\ldots,Q_N)$ and $C'=(C_1,\ldots,C_n)$ would yield:

$$C_i^{(f)} = C_i^{(f)}(Q, C, \Delta t, T) \quad [6]$$

223

224 The assessment of SPM fluxes ($F_{N,f}$) from the source data (*Q'*, *C'*) under experimental conditions (Δt,
225 *T*) is a two-stage process that first solves the inverse problem by fitting the optimal {*p*} parameter set
226 in the *C*(*Q*) model (rating curve) and subsequently uses it for direct calculations by means of [4]:

$$(Q, C, \Delta t, T) \rightarrow \{p\} \rightarrow F_{N,f} \quad [7]$$

227 Most of the time, at least in the French river surveillance network, the intervals between *C* samplings
228 are only approximately regular such that $\Delta t\sim$ should be used instead of Δt. The present procedure is
229 assumed to be valid if the average of the $\Delta t\sim$ values over the data collection period remains
230 sufficiently close to Δt. In other words, this hypothesis is intended to authorise random fluctuations
231 of $\Delta t\sim$ around $\Delta t=T/n$ and is not assumed to hold for drastic changes in data collection strategy.

232

Author-produced version of the article published in Journal of Hydrology, 2014, N°508, p. 364-373
The original publication is available at http://www.sciencedirect.com
Doi: 10.1016/j.jhydrol.2013.10.057

The objective of Step 1 is to test the combined effects of systematic biases in Q' with random errors on C', thus maintaining the optimal conditions of data collection: daily discharge and concentration data over several years. Emphasis is placed on the effects of degraded data quality on both the fitted parameters and the estimated SPM fluxes for the classical ($C=aQ^b$) and improved ($C=aQ^b+a_1\delta S$) rating curves.

Five systematic relative errors in the discharge measurements are addressed and are noted as Q_r = -20%, -10%, 0%, +10% and +20%: if Q^* is the measured dataset and Q' is the collection of exact values, the listed Q_r cases are also written as Q^*/Q'=0.8, 0.9, 1.0, 1.1 and 1.2, respectively. However, random relative errors in the concentration measurements (C^R) were assumed as uniformly distributed within the [-30%, +30%] interval around the collected data. This random treatment involved replicating each station in Table 1 into 100 virtual stations with the intended perturbations in the C data.

The selected objectives are to study the relative variations of the parameters $\{p_r\}$ and those of the calculated SPM fluxes. The latter appear in more eloquent representations when displaying the ratios of calculated and exact fluxes such that the stages of the test procedure may be summarised in:

$$\left(Q_r, C^R\right) \rightarrow \{p_r\} \rightarrow F_{N,f} / F \qquad [8]$$

where the expected results are the mean variation trends in function of Q_r values with dispersion effects arising from the randomised C^R concentration data. The $\{p_r\}$ set is $\{a_r, b_r\}$ for the classical rating curve and $\{a_r, b_r, a_{1r}\}$ for the IRCA.

Step 2 focuses on the effects of the sampling frequencies, especially those with increasing time intervals between C data, while ensuring that the data quality is unaffected, thus producing error-free Q and C data. Numerous combinations of (Δt^R, T_C) values have been tested, where Δt^R designates an average sampling interval affected by a "small" random perturbation (at most equal to

Author-produced version of the article published in Journal of Hydrology, 2014, N°508, p. 364-373
The original publication is available at http://www.sciencedirect.com
Doi: 10.1016/j.jhydrol.2013.10.057

258 $\Delta t/2$), and T_C is the total period of data collection. The Δt^R treatment is the approach chosen to
259 account for the irregular Δt~ intervals previously mentioned. The targets are once again the relative
260 variations and dispersions of the SPM fluxes, as shown in the ratios of calculated and exact fluxes:

$$\left(\Delta t^R, T_C\right) \rightarrow F_{N,f}/F \quad [9]$$

261

262 Step 3 analyses the combined effects of the degraded *Q*-*C* data quality and infrequent *C*
263 measurements on the calculated SPM fluxes within the following procedure:

$$\left(Q_r, C^R, \Delta t^R, T_C\right) \rightarrow F_{N,f}/F \quad [10]$$

264

265 Finally, step 4 provides an application of the IRCA around the estimation of SPM exports from French
266 rivers to the sea. Contrary to the preceding sections, *F* is unknown and is thus estimated from
267 "confidence intervals" around the $F/F_{N,f}$ ratios by relying on the calculated $F_{N,f}$ fluxes.

268

269

Author-produced version of the article published in Journal of Hydrology, 2014, N°508, p. 364-373
The original publication is available at http://www.sciencedirect.com
Doi: 10.1016/j.jhydrol.2013.10.057

3. Results and discussion

3.1 Step 1: Effects of data uncertainty on the calculated SPM fluxes

Effects of data uncertainty on the fitted parameters

Theoretical predictions are available from the scale-invariant properties of the $C=aQ^b$ law: the law should still hold with a modified pre-factor (a^* instead of a) and unchanged exponent (b) when modifying the argument, i.e., measuring Q^* instead of the real Q value:

$$C = aQ^b = a\left(\frac{Q}{Q^*}Q^*\right)^b = a^*Q^{*b} \quad [11]$$

with $a^*=a(Q/Q^*)^b$.

For example, the underestimation of Q by 20% (Q_r = -20%) corresponds to Q^*/Q = 0.8, thus Q/Q^* = 1.25 and a^*/a = $(1.25)^b$. A numerical application with a typical b value of 0.85 yields a^*/a=1.21. In such a case, a relative variation a_r = +21% is theoretically expected. Similar predictions are available for the other tested Q_r values and are represented by the "Theory" dotted lines in Figure 3. Because the b exponent is supposedly unaffected, its relative variation b_r should be zero. No such prediction is available for a_1 and a_{1r}.

[FIGURE 3 ABOUT HERE]

Figure 3 gathers the a_r, b_r and a_{1r} variations; the latter is specific to the $C=aQ^b+a_1\delta S$ model, and the former two are common with the $C=aQ^b$ model. All curves display the global averages of a_r, b_r or a_{1r} for the 22 stations listed in Table 1, and each one is replicated into 100 virtual stations to satisfy the

Author-produced version of the article published in Journal of Hydrology, 2014, N°508, p. 364-373
The original publication is available at http://www.sciencedirect.com
Doi: 10.1016/j.jhydrol.2013.10.057

random procedure on *C* data. Taking the example of a_r, the upper (+) and lower (-) limits of the dispersion envelope are plotted as:

$$a_r^{\pm}(Q_r) = \frac{a^*(Q_r) \pm 1.73\,\sigma_{a^*}(Q_r)}{a} = a_r(Q_r) \pm 1.73\,\frac{\sigma_{a^*}(Q_r)}{a} \quad [12]$$

where σ_{a^*} is the standard deviation in the a^* values and all quantities are functions of Q_r except a, which is the reference value obtained for $Q_r = 0$. The σ_{a^*}/a term is a normalised standard deviation.

The 1.73 factor is usually associated with a 100%-confidence interval for uniform random distributions: once the average value (AV) and standard deviation (σ) are known, the real value falls in the [AV-1.73 σ, AV+1.73 σ] interval. In this work, the uniform random distribution C^R results in nearly uniform random distributions of $a^*(Q_r,C^R)$ and $a_r(Q_r,C^R)$ values for each Q_r value, thus ensuring the validity of the calculated dispersion envelope for $a_r(Q_r,C^R)$. The same procedure applies to parameters *b* and a_1.

Figures 3a, d and g examine the $a_r(Q_r)$ trends and compare them with the theoretical predictions for increasing values of the PEST coefficient of determination (*R*). The atypical non-monotonous variation displayed in Figure 3a is essentially due to poorly fitted data ($R \approx 0.2$) from stations 14, 16, 18 and 19 in Table 1. At such low *R* values, equifinality unavoidably exists such that completely different (*a*, *b*) couples lead to similar performances in the optimisation. For the cited stations, unexpectedly high *a* values compensate for the effects of notably low $b \ll 1$ values, yielding *R* values otherwise obtained from (*a*, *b*) couples with $b \approx 1$.

In Figure 3a, d and g, the dispersion decreases with increasing *R* values and remains limited in the sense that variability is explained by the $a_r(Q_r)$ trends rather than by the "orthogonal" dispersive random effects. As expected, the $a_r(Q_r)$ curves best match the theoretical curves for increasing *R*

Author-produced version of the article published in Journal of Hydrology, 2014, N°508, p. 364-373
The original publication is available at http://www.sciencedirect.com
Doi: 10.1016/j.jhydrol.2013.10.057

values, which indicate a clearer power-law organisation of the dataset. Unfortunately, only 7 stations are encompassed by the R>0.65 criteria vs. 17 stations out of 22 for R>0.3.

Rather weak dispersions and low b_r values (i.e., nearly unchanged b exponents) in Figure 3b, e, and h appear to be in good agreement with expectations arising from the scale-invariance properties of power laws. However, a striking feature is the increasing variability of a_r and b_r with decreasing determination values. The underlying and unanswered question at this point is whether this variability will endanger the reliability of SPM flux calculations for fittings with low determination values. This question is the subject of the advocated "composite analysis" performed in the following paragraphs, from data uncertainty to uncertainty in the fitted parameters as well as in the calculated fluxes.

The a_{1r} variations (Figure 3c, f and i) also show limited dispersion, except for strong discharge underestimations. Positive relative errors in the discharge (Q_r>0) cause positive relative variations in the a_1 coefficient (a_{1r}>0). A key point is that the δS term is identical regardless of the Q_r value because the q/Q_0 ratio is used in [1], where both q and Q_0 are affected by the same relative error in the discharge values. This choice of δS, referred to as "identical by construction", allows direct interpretation of the role played by a_1: the $a_1\delta S$ correction behaves similar to a_1, producing its strongest relative variations (a_{1r}=-30%) for the strongest discharge underestimations (Q_r=-20%).

Effects of data uncertainty on the calculated SPM fluxes

Contrary to the fitted coefficients, the calculated SPM fluxes exhibit almost no dependence on the determination (R) values. Therefore, Figure 4 plots the SPM fluxes and dispersions obtained for all R values. As shown previously, the upper (+) and lower (-) limits of the dispersion envelope are written:

Author-produced version of the article published in Journal of Hydrology, 2014, N°508, p. 364-373
The original publication is available at http://www.sciencedirect.com
Doi: 10.1016/j.jhydrol.2013.10.057

$$\left(\frac{F_{N,f}}{F}\right)^{\pm}(Q_r)=\frac{F_{N,f}(Q_r)\pm 1.73\sigma_{F_{N,f}}(Q_r)}{F}=\left(\frac{F_{N,f}}{F}\right)(Q_r)\pm 1.73\frac{\sigma_{F_{N,f}}(Q_r)}{F} \quad [13]$$

341

342 [FIGURE 4 ABOUT HERE]

343

344 Figure 4a and b show weak dispersions and similar variation trends because the calculated SPM
345 fluxes increase with the estimated discharge values. The relative variations in the calculated fluxes
346 are near-linear functions of the systematic relative error present in the discharge measurements for
347 both the classical $C=aQ^b$ (Figure 4a) and the improved $C=aQ^b+a_1\delta S$ (Figure 4b) rating curves. The
348 difference between these parallel curves is the "offset" added in Figure 4b by the $a_1\delta S$ correction,
349 which perfectly remedies the underestimation due to the classical method. The gain obtained from
350 the $a_1\delta S$ correction is approximately 5% along the "calculated on exact" vertical axis, with even
351 weaker dispersion in the results. For example, if the discharge is known with a 10% uncertainty (5%
352 on each side of the Q_r=0 line), then $F_{N,f}/F$ lies within the 0.88-1.04 and 0.93-1.07 ranges of the
353 classical and improved rating curves, respectively.

354

355 Looking at the nearly stable *b* values ($b_r \approx 0$ in Figure 3b, e and h), it is worth noting that increases in
356 the fitted *a* values ($a_r > 0$ in Figure 3d and g) were not sufficient to counterbalance the influence of
357 the discharge underestimations ($Q_r < 0$). The calculated fluxes still underestimate the real values
358 when the discharge is underestimated for both methods in Figure 4. However, the overall effect of
359 the storage term is an increase in the calculated ($F_{N,f}$) SPM fluxes, which is validated by
360 improvements of approximately 5% in the determination values.

361

362 *3.2 Step 2: Effects of data infrequence on the calculated SPM fluxes*

363

Author-produced version of the article published in Journal of Hydrology, 2014, N°508, p. 364-373
The original publication is available at http://www.sciencedirect.com
Doi: 10.1016/j.jhydrol.2013.10.057

364 This subsection leaves data quality concerns aside to focus on data availability, especially on the
365 problem of infrequent *C* data. This subsection also tackles the sampling frequency issue by
366 addressing the interplay between the number (*n*) of available data, the total collection period (*T*) and
367 the sampling period (Δt), as commented next to [6]. As previously mentioned, the sampling periods
368 have always been tested with slight random perturbations (Δt^R) of the predefined values to account
369 for more realistic field conditions, resulting in approximations (Δt~) of the predefined Δt intervals.
370 Figure 5 displays the ratio of the calculated and exact SPM fluxes, the medians of the absolute errors
371 on this ratio and the statistics for the absolute errors on this ratio in the Δt~30 day case for various
372 (*n*, *T*, Δt) triplets, thus allowing comparisons between the fitted $C=aQ^b$ and $C=aQ^b+a_1\delta S$ models.
373
374 [FIGURE 5 ABOUT HERE]
375
376 Figure 5a targets the evolution of the "calculated on exact" ratios of SPM fluxes for decreasing values
377 of the sampling interval (Δt) and also shows the positive impact of increasingly long periods of data
378 collection (*T*) for the given sampling intervals. A clear increase in dispersion occurs for Δt>5 days
379 combined with *T*<4 years. Further on the left of the diagram, the rather typical monthly sampling
380 period (Δt~30 days) requires at least an 8-year collection period (*T*=8 years) for the "calculated on
381 exact" ratios to lie within the gross [0.5, 5.0] interval. Figure 5b also begins with highly dispersed
382 values for combinations of high sampling periods, even with long collection periods, and exhibits
383 additional oscillations before achieving convergence because it is obviously more seriously affected
384 by weak *T* values. The main difference is the highest dispersion for Δt~5 days and *T*=4 years and for
385 Δt~20 days and *T*=8 years. A common point appears to be the trend of overestimating the exact SPM
386 fluxes, even for the most relevant estimations that rely on low Δt and high *T* values.
387
388 A complementary view is given by Figure 5c and d and shows the median of the absolute error of the
389 calculated against exact ratio as a function of the number of available concentration data (*n*) by

Author-produced version of the article published in Journal of Hydrology, 2014, N°508, p. 364-373
The original publication is available at http://www.sciencedirect.com
Doi: 10.1016/j.jhydrol.2013.10.057

plotting a dedicated curve for each of the total tested collection periods (T=1, 4, 8, 12 and 15 years). Figure 5c shows that n=150 takes the error under 20%, whereas n=300 is required for errors lower than 10%. These results are nearly independent of T and thus hold for sampling intervals $\Delta t=T/n$ with n above the mentioned thresholds. For example, it takes Δt~20 days for T=8 years to dispose of n=150 concentration data. Equivalently, T=13.7 years is the minimum time period required to fulfil the 20% error criterion when performing monthly samplings (Δt~30 days). By contrast, the trends in Figure 5d are less uniform because the error values exhibit a clear dependence on the T values, which calls in question analyses that only involve the number n of concentration data and make a case for combined (n, T) criteria. For example, n>200 and T≥8 years will confine the relative error to under the 20% mark. For monthly samplings, the n>200 threshold alone corresponds to T>18 years, which *de facto* verifies T≥8 years. This result tends to indicate that the condition for the number of data remains the most restrictive and could still be maintained alone.

Figures 5e and f focus on the case of monthly concentration samplings. The monotonic and exponential-like decrease of the error in Figure 5e emphasises the regular gain in the stability of the $C=aQ^b$ method for total data collection periods increasing from T=1 to 15 years. Figure 5f shows the same trend with a few irregularities. The dynamic definition chosen for the storage term (S) and its variations (δS) plausibly requires sufficiently dense concentration data for significant gains in precision, with potentially better performances than the $C=aQ^b$ method but apparently with slightly more restrictive conditions of application.

3.3 Step 3: Combined effects of data uncertainty and infrequence on the calculated SPM fluxes

Subsection 3.1 established the ability of the $C=aQ^b+a_1\delta S$ model to better predict the SPM fluxes, as compared with the $C=aQ^b$ model, using degraded-quality data. Subsection 3.2 showed that the $C=aQ^b+a_1\delta S$ model was slightly more sensitive to data infrequence. The present subsection tests both

Author-produced version of the article published in Journal of Hydrology, 2014, N°508, p. 364-373
The original publication is available at http://www.sciencedirect.com
Doi: 10.1016/j.jhydrol.2013.10.057

models against combined data uncertainty and infrequence to simulate eventual real-life conditions: systematic relative errors in the discharge measurements (poorly-gauged stations), random errors in the concentration measurements (uncertain techniques) and possibly sparse concentration measurements (limited credits).

Figure 6 uses the 100%-confidence intervals, similar to these already defined in [12] and [13], to draw dispersion envelopes associated with the random treatment of concentration data for daily (Δt~1 day), decadal (Δt~10 days) and monthly (Δt~30 days) concentration samplings. The Δt~1 day case corresponds to the results shown in Figure 4. In Figure 6, sparser concentration samplings lead to wider dispersion envelopes that are somewhat shifted towards higher flux predictions. The drift and dispersion are a bit more pronounced for the storage method with too many data lacking, although the curves are quite similar between sketches (a) and (b). Figure 6 also proves that infrequent and limited-quality data may still be used for flux predictions (at least with caution and while staying within the tested ranges for errors) because they do not lead to completely divergent, uncontrolled or unpredictable results.

[FIGURE 6 ABOUT HERE]

As a mean behaviour among all stations, if one commits a systematic relative error within the [-5%, +5%] interval on *Q* together with a random relative error within the [-30%, +30%] interval on *C* while only disposing of *C* data each 30 days on average, the calculated SPM flux still lies within a factor of 0.60-1.60 of the real value with the classical rating curve. The improved rating curve gives the estimation in the 0.65-1.65 range. A narrower 0.80-1.40 range would be obtained if considering 60%-confidence intervals instead of 100%-confidence intervals. The following subsection therefore addresses possible applications in bounding sediment budgets.

Author-produced version of the article published in Journal of Hydrology, 2014, N°508, p. 364-373
The original publication is available at http://www.sciencedirect.com
Doi: 10.1016/j.jhydrol.2013.10.057

442 *3.4 Step 4: Application to sediment exports from French rivers*

443

444 In real-life situations, the predicted flux is known, and the objective is to define a plausible interval
445 for the real flux. This process may be carried out by examining the "exact against calculated" ratios
446 along the y-axis instead of the "calculated against exact" ratios shown in the previous figures. Figure
447 7a presents dispersion envelopes corresponding to the 100%-confidence intervals, indicating where
448 the exact SPM flux may lie for sampling periods of Δt~10 days and Δt~30 days. Taking a 10%
449 uncertainty for the discharge measurements (between -5 and +5%), retaining the 60% random
450 uncertainty in the concentration data (between -30% and +30%) and assuming a worst-case sampling
451 interval of Δt~30 days for the concentration data, the real flux (F) lies between 0.6 and 1.53 times the
452 calculated value ($F_{N,f}$).

453

454 In the French sediment budget proposed by Delmas et al. (2012) for the major rivers to the sea, the
455 calculations were performed from monthly sediment concentration samplings (Δt~30 days) over
456 more than 25 years, except for the Rhone river, for which daily measurements were available in
457 certain periods, yielding an average of Δt~10 days. Figure 7b shows the induced uncertainty in the
458 calculated sediment fluxes. The estimated total sediment load for the selected rivers is 13.9 Mt/yr.
459 From the uncertainties calculated in this work, the real sediment export from these rivers is
460 contained between 10.05 Mt/yr and 17.7 Mt/yr.

461

462 [FIGURE 7 ABOUT HERE]

463

464

Author-produced version of the article published in Journal of Hydrology, 2014, N°508, p. 364-373
The original publication is available at http://www.sciencedirect.com
Doi: 10.1016/j.jhydrol.2013.10.057

4. Conclusion

This paper tackled feasibility and precision issues in calculation of fluxes of suspended particulate matter (SPM) by assuming systematic errors in the water discharge (Q) and random errors in sediment concentration (C) data and under the additional constraint of infrequent sediment concentration samplings. The chosen framework compared the merits and drawbacks of the classical rating curve ($C=aQ^b$) with those of an improved rating curve approach (IRCA, $C=aQ^b+a_1\delta S$) in which the correction term is an indicator of the variations in sediment storage and is thus related to flow dynamics. Successive steps of the analysis were: (1) to establish the effects of data uncertainty on the fitted coefficients (a, b, a_1) and on the calculated SPM fluxes, (2) to examine how infrequent sediment concentration data affects these estimates and (3) to combine both effects into the definition of realistic cases, thus allowing an application to sediment exports from French rivers.

Step 1 involved systematic relative errors in the flow discharge (-20%, -10%, 0%, +10%, +20%) and random relative errors in the sediment concentration in the [-30%, +30%] interval. Increasing a values and stable b values were observed when gradually moving from -20% to +20% errors in the discharge, together with decreasing dispersion in the fitted (a, b) coefficients with the increasing goodness-of-fit. Such results globally meet the expectations arising from the scale-invariant properties of power laws. As a complement, the dispersion in the magnitude of the $a_1\delta S$ correction term appeared far stronger for the most severe discharge underestimations than for all other tested errors. The general trend was that of an upward correction due to the $a_1\delta S$ term: the IRCA remedies the small systematic underestimations observed with the classical rating curve method. The IRCA always performs better than the classical rating curve (and does not require additional information) when frequent concentration measurements are available, regardless of the period of data collection and the tested errors in the discharge and concentration.

Author-produced version of the article published in Journal of Hydrology, 2014, N°508, p. 364-373
The original publication is available at http://www.sciencedirect.com
Doi: 10.1016/j.jhydrol.2013.10.057

Step 2 hypothesised error-free discharge and concentration measurements to focus on the effects of sampling frequencies on the calculated sediment fluxes. The results show that the number (n) of available C measurements is more discriminating than the sampling frequency itself, at least within the tested data collection strategies, and the provided data measurements captured sufficient variability in the river behaviour according to the Wilcoxon test of data representativity. The criteria on *n* were revealed as the most restrictive with respect to the performances of the rating curves: *n*>200 guaranteed that the calculated SPM fluxes would lie within the [-20%, +20%] interval around the exact values.

Step 3 consisted of combining the previous aspects and checking whether degradation of the results remained progressive and controlled, or if data uncertainty and infrequence would yield diverging results and render the methods inapplicable. This question was especially pertinent for the IRCA, that was slightly better in dealing with uncertain data but was slightly more sensitive to data infrequence. Bounding the calculated SPM fluxes within the confidence intervals around the real values allowed the following observations: the calculations are slightly higher with the improved rating curve, and the dispersion also grows slightly wider with increasing errors in discharge, but the results always stay within the acceptable margins of errors.

In the chosen worst-case scenario, poor sampling intervals of 30 days (on average) over approximately fifteen years combined with relative errors in discharge between -5% and +5% and random errors within the [-30%, +30%] interval for the sediment concentration values resulted in calculated fluxes that are still bounded within a factor of 0.60 to 1.65 of the real values. However, all other realistic cases yield far better estimates. For example, there is no technical improvement, but a shorter 5-day sampling interval on average reduces the relative error to below 10%. Finally, the application to French rivers illustrated the reliability of the method for a wide variety of irregular sampling intervals and flow discharge and sediment concentration ranges, provided that sufficient

Author-produced version of the article published in Journal of Hydrology, 2014, N°508, p. 364-373
The original publication is available at http://www.sciencedirect.com
Doi: 10.1016/j.jhydrol.2013.10.057

concentration data were available. In addition to technical improvements, a key issue is to better address the irregular samplings and thus to extract additional information from the discharge dynamics, especially the antecedent flow conditions, through ongoing developments around the sediment storage term in the IRCA.

In its present formulation, the IRCA perfectly corrects the known underestimation of the classical rating curve, if frequent concentration samplings are available, combined with the uncertainties of discharge and concentration values. Both methods perform well when concentration samplings become sparse if the sampling period and number of concentrations remain sufficiently large. Finally, only the IRCA is subject to improvements for better exploitation of the information contained in the temporal dynamics of discharge.

Acknowledgment

The authors would like to acknowledge the financial support of the PIREN Seine Program and the support and constructive comments of Xavier Bourrain and Jean-Noel Gautier of the AELB.

Author-produced version of the article published in Journal of Hydrology, 2014, N°508, p. 364-373
The original publication is available at http://www.sciencedirect.com
Doi: 10.1016/j.jhydrol.2013.10.057

534 **References**

535

536 Asselmann, N. E. M., 2000. Fitting and interpretation of sediment rating curves, *Journal of Hydrology*,
537 234, pp.228-248.

538

539 Clauset, A., Shalizi, C. R., Newman, M. E. J., 2009. Power-law distribution in empirical data, *Society for*
540 *Industrial and Applied Mathematics – Review*, 51 (4), pp.661-703.

541

542 Coynel, A., Schäfer, J. Hurtrez, J. E., Dumas, J., Etcheber, H., Blanc, G., 2004. Sampling frequency and
543 accuracy of SPM flux estimates in two contrasted drainage basins. Science of the Total Environment
544 330, pp.233–247.

545

546 Delmas, M., Cerdan, O., Mouchel, J. M., Garcin, M., 2009. A method for developing large-scale
547 sediment yield index for European river basins, Journals of Soils and Sediments, 9 (6), pp.613-626.

548

549 Delmas, M., Cerdan, O., Cheviron, B., Mouchel, J.-M., 2011. River basin sediment flux assessments,
550 *Hydrological Processes*, 25 (10), pp.1587-1596.

551

552 Delmas, M., Cerdan, O., Cheviron, B., Mouchel, J.-M., Eyrolle, F., 2012. Sediment exports of French
553 rivers to the sea, *Earth Surface Processes and Landforms*, 37 (7), pp.754-762.

554

555 Doherty, J., (2004). PEST – Model-independent parameter estimation, User Manual, Watermark
556 Numerical Computing.

557

558 Ferguson, R. I., 1986. River loads underestimated by rating curves, *Water Resources Research*, 22 (1),
559 pp.74-76.

Author-produced version of the article published in Journal of Hydrology, 2014, N°508, p. 364-373
The original publication is available at http://www.sciencedirect.com
Doi: 10.1016/j.jhydrol.2013.10.057

Ferguson, R. I., 1987. Accuracy and precision of methods for estimating river loads, Earth Surface Processes and Landforms, 12 (1), pp.95-104.

Goldstein, M. L., Morris, S. A., Yen, G. G., 2004, Problems with fitting to the power law distribution, *European Physical Journal B*, 41 (2), pp.255-258.

Horowitz, A. J., 1997. Some thoughts on problems with various samplings media used for environmental monitoring, Analyst, 122, pp.1193-1200.

Horowitz, A. J., Elrick, K. A. and Smith, J. J., 2001. Estimating suspended sediment and trace element fluxes in large river basins: methodological considerations as applied to the NASQAN programme, *Hydrological Processes*, 15, pp.1107-1132.

Horowitz, A. J., 2003. An evaluation of sediment rating curves for estimating suspended sediment concentration for subsequent flux calculation, *Hydrological Processes*, 17, pp.3387-3409.

Laherrere, J., 1996. "Parabolic fractal" distributions in nature, *Comptes-Rendus de l'Académie des Sciences – 2A Sciences de la Terre et des Planètes*, 322 (7), pp.535-541.

Laherrere, J., Sornette, D., 1998. Stretched exponential distributions in nature and economy: "fat tails" with characteristic scales, *European Physical Journal B*, 2 (4), pp.525-539.

Ludwig, W., Probst, J. L., 1998. River sediment discharge to the oceans: present-day controls and global budgets, *American Journal of Science*, 298, pp.265-295.

Author-produced version of the article published in Journal of Hydrology, 2014, N°508, p. 364-373
The original publication is available at http://www.sciencedirect.com
Doi: 10.1016/j.jhydrol.2013.10.057

586 Mano, V., Nemery, J., Belleudy, P. and Poirel, A., 2009. Assessment of suspended sediment transport
587 in four alpine watersheds (France): influence of the climatic regime, *Hydrological Processes*, 23,
588 pp.777-792.
589
590 Meybeck, M., Laroche, L., Durr, H. H. and Syvitski, J. P. M., 2003. Global variability of daily total
591 suspended solids and their fluxes in rivers, *Global and Planetary Change*, 39, pp.65-93.
592
593 Mitzenmacher, M., 2004. A Brief history of generative models for power law and lognormal
594 distributions, *Internet Mathematics*, 1 (2), pp.226-251.
595
596 Moatar, F., Meybeck, M., Raymond, S., Birgand, F., Curie, F. (2012). River flux uncertainties predicted
597 by hydrological variability and riverine material behavior, *Hydrological Processes*, DOI:
598 10.1002/hyp.9464.
599
600 Moatar, F., Meybeck, M., 2005. Compared performance of different algorithms for estimating annual
601 loads flows by the eutrophic River Loire, *Hydrological Processes*, 19, pp.429-444.
602
603 Morgan, R.P.C., 1995. Soil erosion and conservation, 2nd ed., Longman, London.
604
605 Newman, M. E. J., 2005. Power laws, Pareto distributions and Zipf's law, *Contemporary Physics*, 46
606 (5), pp.323-351.
607
608 Peters-Kümmerly, B.E., 1973. Untersuchungen über Zusammensetzung und Transport von
609 Schwebstoffen in einigen Schweizer Flüssen, *Geographica Helvetica*, 28, pp.137–151.
610

Author-produced version of the article published in Journal of Hydrology, 2014, N°508, p. 364-373
The original publication is available at http://www.sciencedirect.com
Doi: 10.1016/j.jhydrol.2013.10.057

611 Phillips, J. M., Webb, B. W., Walling, D. E., Leeks, G. J. L., 1999. Estimating the suspended sediment
612 loads of rivers in the LOIS study area using infrequent samples, *Hydrological Processes*, 13, pp.1035-
613 1050.
614
615 Picouet, C., Hingray, B. and Olivry, J. C., 2001. Empirical and conceptual modeling of the suspended
616 sediment dynamics in a large tropical African river: the Upper Niger river basin, Journal of Hydrology,
617 250, pp.19-39.
618
619 Quilbé, R., Rousseau, A. N., Duchemin, A., Poulin, A., Gangbazo, G., Villeneuve, J. P., 2006. Selecting a
620 calculation method to estimate sediment and nutrient loads in streams: application to the
621 Beaurivage River (Québec, Canada), Journal of Hydrology, 326, pp.295-310.
622
623 Rode, M., Suhr, U., 2007. Uncertainties in selected river quality data. Hydrol. Earth Syst. Sci., 11,
624 pp.863-874.
625
626 Smart, T. S., Hirst, D. J. and Elston, D. A., 1999. Methods for estimating loads transported by rivers,
627 *Hydrology and Earth System Sciences*, 3 (2), pp.295-303.
628
629 Sornette, D., 2006, Critical Phenomena in Natural Sciences: chaos, fractals, self-organization and
630 disorder (Springer, Berlin), chapter 14, 2nd edition, 444p.
631
632 Walling, D. E., Webb, B. W., 1981. The reliability of suspended sediment load data, In *Erosion and*
633 *Sediment Transport Measurement*, IAHS Publication No 133, IAHS Press: Wallingford; pp.177-194.
634
635 Walling, D. E., Webb, B. W., 1985. Estimating the discharge of contaminants to coastal rivers: some
636 cautionary comments, *Marine Pollution Bulletin*, 16, pp.488-492.

Author-produced version of the article published in Journal of Hydrology, 2014, N°508, p. 364-373
The original publication is available at http://www.sciencedirect.com
Doi: 10.1016/j.jhydrol.2013.10.057

637

638 Walling, D. E., Fang, D., 2003. Recent trends in the suspended sediment loads of the World's rivers,

639 *Global and Planetary Change*, 39, pp.111-126.

640
641

Author-produced version of the article published in Journal of Hydrology, 2014, N°508, p. 364-373
The original publication is available at http://www.sciencedirect.com
Doi: 10.1016/j.jhydrol.2013.10.057

642 **Table caption**
643
644 Table 1 – Names and locations of the USGS stations used in this study together with the drained
645 areas of the monitored rivers and statistics of their discharge (Q) and concentration (C) values. The
646 Q_0 base-flow limit is an indicator introduced in the IRCA-Improved Rating Curve Approach, and σ(Q)
647 and σ(C) report the standard deviations of the Q and C data, respectively.
648
649

Author-produced version of the article published in Journal of Hydrology, 2014, N°508, p. 364-373
The original publication is available at http://www.sciencedirect.com
Doi: 10.1016/j.jhydrol.2013.10.057

650 **Table 1**

651

USGS station		Drained area	Min Q	Base-flow Q_0	Median Q	Mean Q	Max Q	σ(Q)	Min C	Median C	Mean C	Max C	σ(C)
#	*River name and station location*	*km²*	----------	----------	*m³ s⁻¹*	----------	----------	----------	----------	----------	*g L⁻¹*	----------	----------
1	Rappahannock River at Remington, VA	1603	0.1	17.4	11.2	19.0	1296.9	32.9	1	11	39	2070	105
2	Roanoke River at Randolph, VA	7682	5.1	72.6	49.6	79.3	1996.3	102.1	1	34	76	2060	142
3	Dan River at Paces, VA	6700	6.9	64.4	53.2	77.7	1795.3	91.6	5	60	122	2260	193
4	Yadkin River at Yadkin College, NC	5905	9.3	68.7	62.3	83.7	1868.9	87.0	1	70	150	2970	224
5	Muskingum River at Dresden, OH	15522	13.0	89.1	93.2	165.7	1067.5	177.5	1	30	60	1600	84
6	Muskingum River at McConnelsville, OH	19223	16.1	111.7	171.0	256.6	1350.0	229.7	2	48	77	1710	100
7	Hocking River at Athens, OH	2442	0.7	24.3	9.3	25.0	883.5	49.3	1	14	56	1320	116
8	Scioto River at Highby, OH	13289	7.1	121.6	61.2	133.3	3596.2	196.8	1	41	99	2520	177
9	Little Miami River at Milford, OH	3116	1.5	39.8	17.4	38.6	863.7	59.4	1	40	103	4850	216
10	Great Miami River at Sydney, OH	1401	0.8	10.0	6.7	15.9	250.3	23.6	1	50	72	1710	98
11	Stillwater River at Pleasant Hill, OH	1303	0.3	14.5	4.0	12.2	373.8	25.6	1	23	52	1970	108
12	Maume River at Waterville, OH	16395	0.5	95.0	53.0	148.6	3199.8	247.7	1	39	82	2240	129
13	Upper Iowa River near Dorchester, IA	1994	2.2	9.1	7.4	12.7	268.2	17.5	1	43	192	10000	677
14	Iowa River at Iowa City, IA	8472	1.4	21.2	37.9	64.0	410.6	65.2	1	55	103	7540	215
15	Des Moines River near Saylorville, IA	15128	0.4	44.9	27.8	69.8	1333.7	109.6	1	120	240	5400	356
16	Des Moines River near Saylorville, IA	15128	2.1	53.4	48.4	101.1	1254.4	129.4	0.7	32	46	1210	51
17	Illinois River at valley City, IL	69264	37.7	3.6	549.3	743.0	3398.0	572.3	13	120	182	3720	202
18	Kaskakia River at Cooks Mills, IL	1225	0.0†	5.8	4.9	12.7	274.4	22.8	1	46	60	1710	67
19	Kaskakia River near Venedy Station, IL	11378	2.0	35.8	53.8	109.3	1379.0	145.5	5	81	124	2590	157
20	Mississipi River at St. Louis, MO	1805222	1166.7	3808.6	4898.8	6154.1	29732.7	3841.3	21	217	340	6720	375
21	Salinas River near Spreckels, CA	10764	0.0‡	16.4	0.2	9.3	1121.3	42.6	1	36	306	24000	1273
22	Sacramento River at Sacramento, CA	60883	112.4	358.2	461.6	656.7	2797.7	495.7	8	47	75	1960	88

† Min Q=0.001 $m^3 s^{-1}$

‡ Min Q=0.01 $m^3 s^{-1}$

Author-produced version of the article published in Journal of Hydrology, 2014, N°508, p. 364-373
The original publication is available at http://www.sciencedirect.com
Doi: 10.1016/j.jhydrol.2013.10.057

652 **Figure captions**

653

654 Figure 1 – Sediment storage index S(t) calculated from discharge values Q(t) and Q_0, in an application
655 to the Hocking River at Athens, Ohio (station 7, Table 1).

656

657 Figure 2 – Simplified flow chart of the fitting procedure.

658

659 Figure 3 – Relative variation and dispersion of the fitted coefficients in $C=aQ^b$ (a, b, d, e, g, h) and
660 $C=aQ^b+a_1\delta S$ models (c, f, i) for increasing values of the coefficient of determination. Dispersion
661 envelopes correspond to the 100% confidence intervals. Lines in the middle of the envelopes show
662 averages over all stations listed in Table 1.

663

664 Figure 4 – Ratios and dispersion of calculated on exact SPM fluxes obtained from the fitted $C=aQ^b$ (a)
665 and $C=aQ^b+a_1\delta S$ models (b) without any criterion for the coefficient of determination. These results
666 were obtained from daily samplings over the entire sampling periods at each USGS station, *i.e.,*
667 station-specific time periods. Dispersion envelopes correspond to the 100% confidence intervals.
668 Lines in the middle of the envelopes show the averages over all stations listed in Table 1.

669

670 Figure 5 – Ratios of calculated on exact SPM fluxes (a, b), medians of the absolute errors of these
671 ratios (c, d) and statistics for the absolute errors of these ratios for sampling periods Δt~30 days (e,
672 f). The results are obtained from the fitted $C=aQ^b$ and $C=aQ^b+a_1\delta S$ models for various combinations
673 involving the number (n) of available concentration data, the total time period for data collection (T)
674 and the sampling period (Δt) for concentration data.

675

676 Figure 6 – Dispersion envelopes for the ratios of calculated and exact SPM fluxes obtained from
677 uncertain and infrequent concentration data by fitting $C=aQ^b$ (a) and $C=aQ^b+a_1\delta S$ models (b). These

Author-produced version of the article published in Journal of Hydrology, 2014, N°508, p. 364-373
The original publication is available at http://www.sciencedirect.com
Doi: 10.1016/j.jhydrol.2013.10.057

678 results were obtained over the entire sampling period at each USGS station, i.e., station-specific time
679 periods. These dispersion envelopes correspond to the 100% confidence intervals averaged over the
680 entire dataset listed in Table 1. Each station has been affected with systematic errors in discharge,
681 random errors in concentration, and increased sampling periods.
682
683 Figure 7 – Dispersion envelopes (100% confidence intervals) for the ratios of exact on calculated SPM
684 fluxes obtained from uncertain and infrequent concentration data by fitting the $C=aQ^b+a_1\delta S$ model
685 (a). Application to sediment exports from French rivers, where inner and outer circles bound the real
686 SPM values (b).
687
688

Author-produced version of the article published in Journal of Hydrology, 2014, N°508, p. 364-373
The original publication is available at http://www.sciencedirect.com
Doi: 10.1016/j.jhydrol.2013.10.057

689 **List of Figures**

690

691 Figure 1:

692

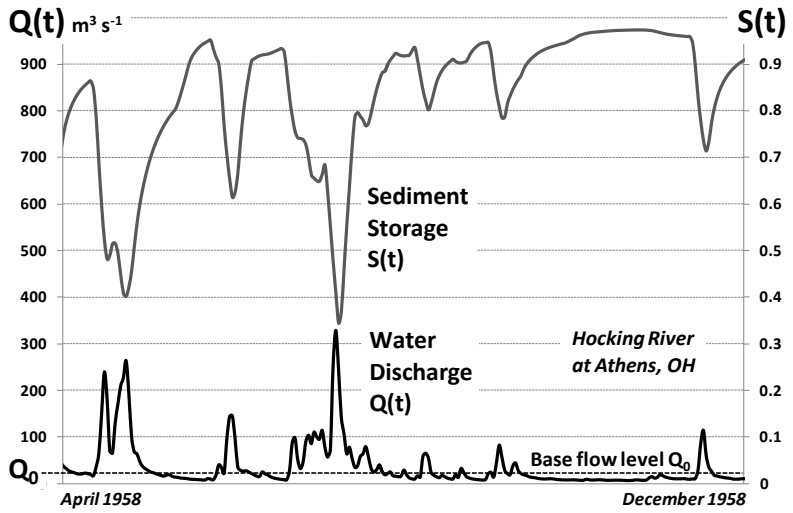

693

694

695

Author-produced version of the article published in Journal of Hydrology, 2014, N°508, p. 364-373
The original publication is available at http://www.sciencedirect.com
Doi: 10.1016/j.jhydrol.2013.10.057

696 Figure 2:
697

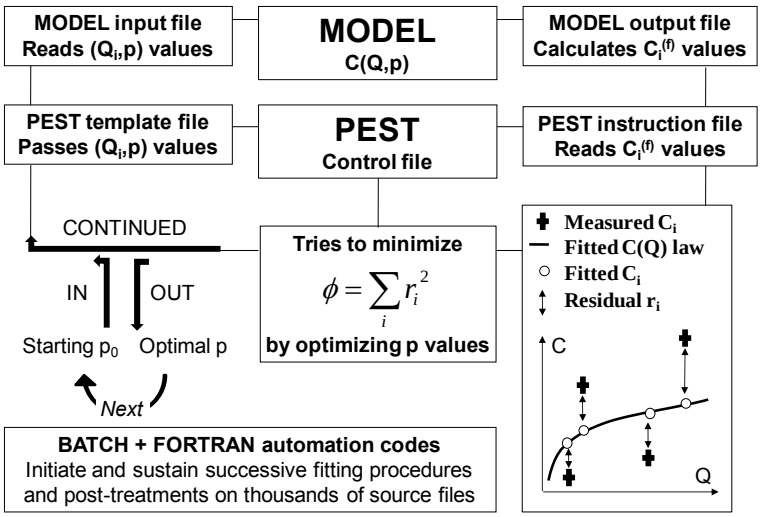

698
699
700

Author-produced version of the article published in Journal of Hydrology, 2014, N°508, p. 364-373
The original publication is available at http://www.sciencedirect.com
Doi: 10.1016/j.jhydrol.2013.10.057

Figure 3:

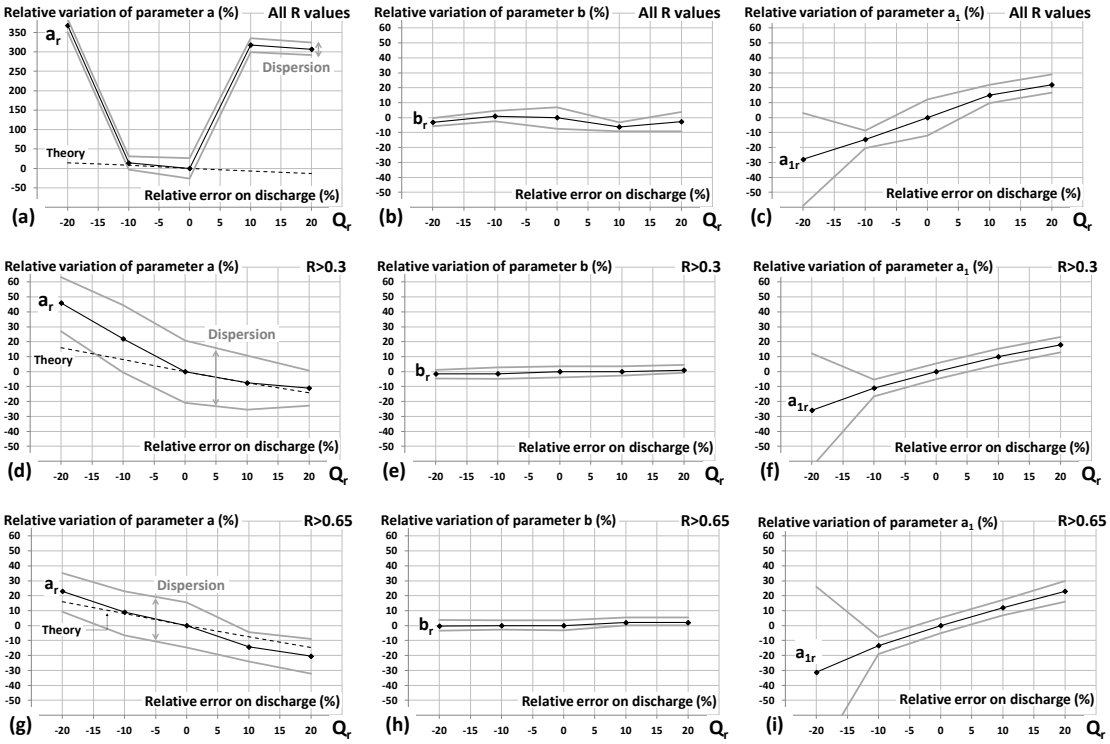

Author-produced version of the article published in Journal of Hydrology, 2014, N°508, p. 364-373
The original publication is available at http://www.sciencedirect.com
Doi: 10.1016/j.jhydrol.2013.10.057

709 Figure 4:
710
711

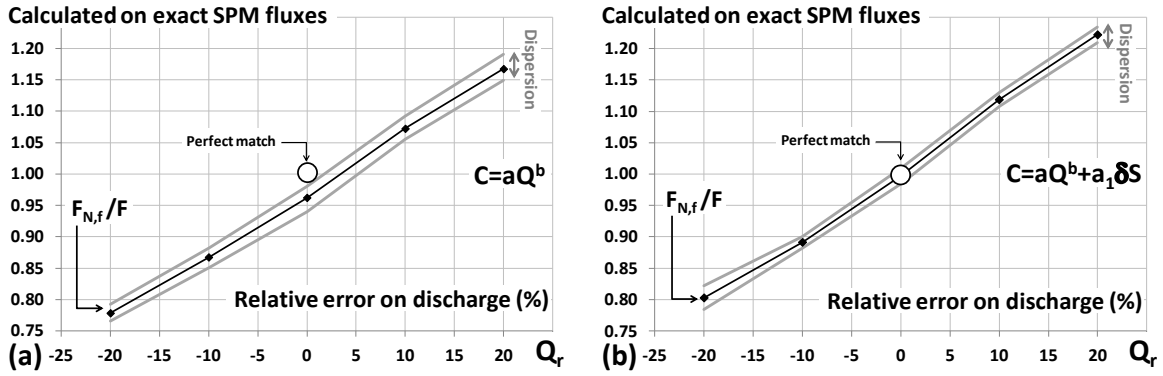

712
713
714

Author-produced version of the article published in Journal of Hydrology, 2014, N°508, p. 364-373
The original publication is available at http://www.sciencedirect.com
Doi: 10.1016/j.jhydrol.2013.10.057

715 Figure 5:
716
717

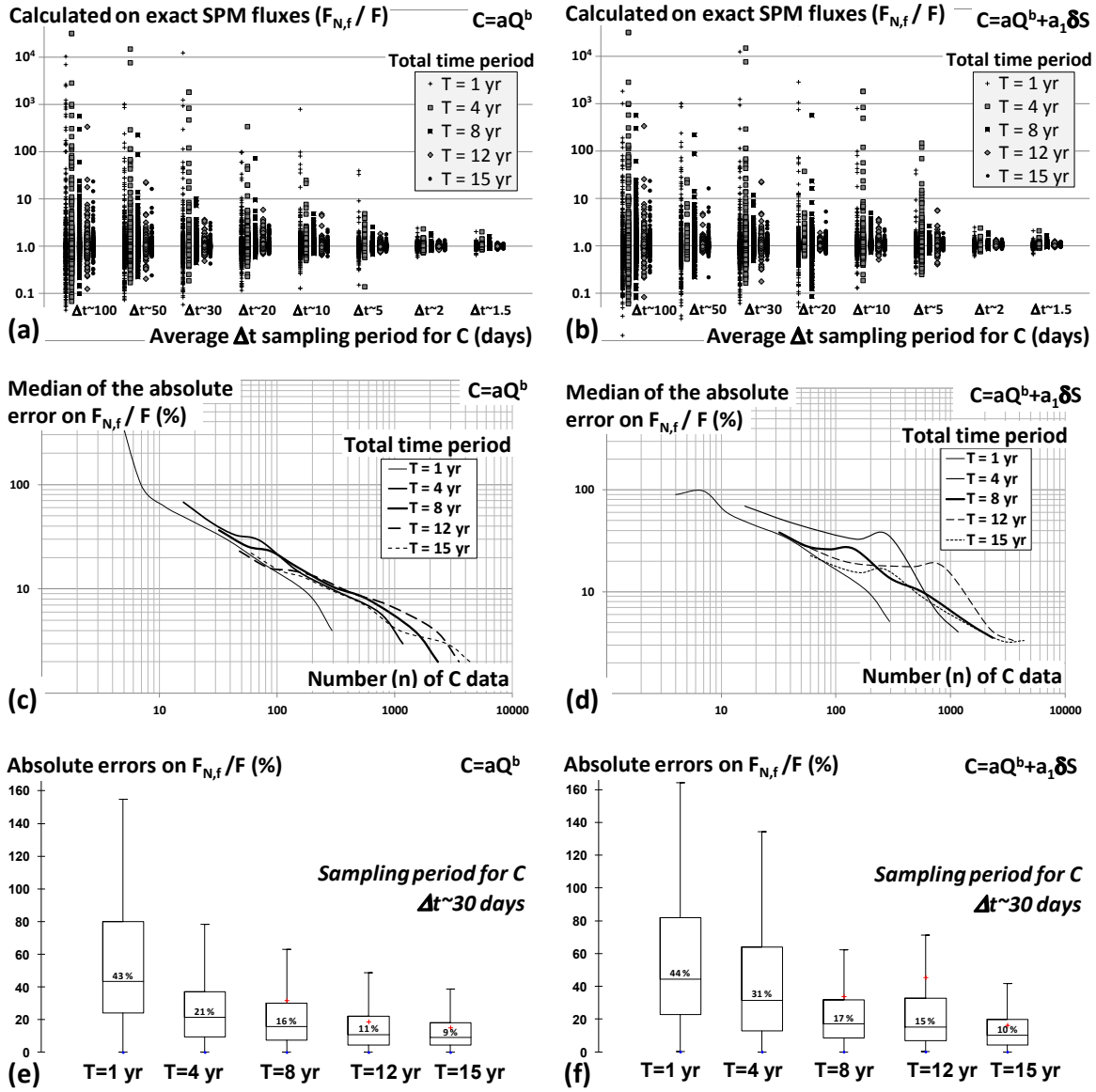

718
719
720
721
722

Author-produced version of the article published in Journal of Hydrology, 2014, N°508, p. 364-373
The original publication is available at http://www.sciencedirect.com
Doi: 10.1016/j.jhydrol.2013.10.057

723 Figure 6:
724

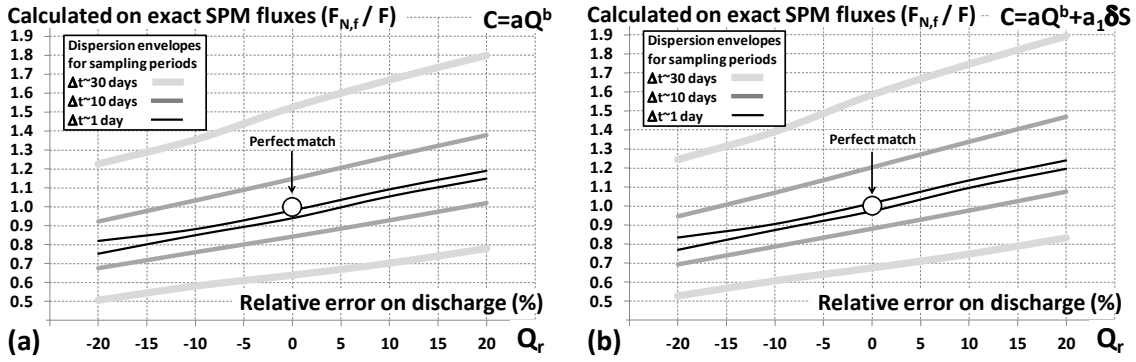

725
726
727

Author-produced version of the article published in Journal of Hydrology, 2014, N°508, p. 364-373
The original publication is available at http://www.sciencedirect.com
Doi: 10.1016/j.jhydrol.2013.10.057

728 Figure 7:
729

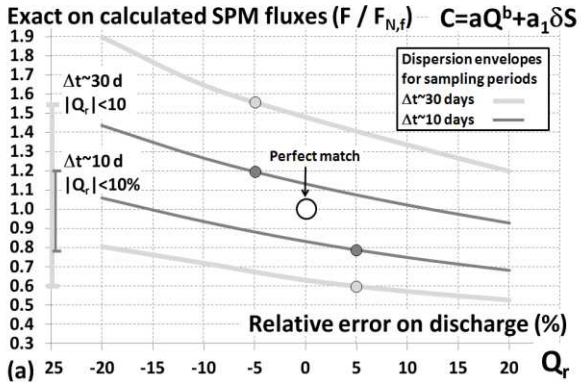

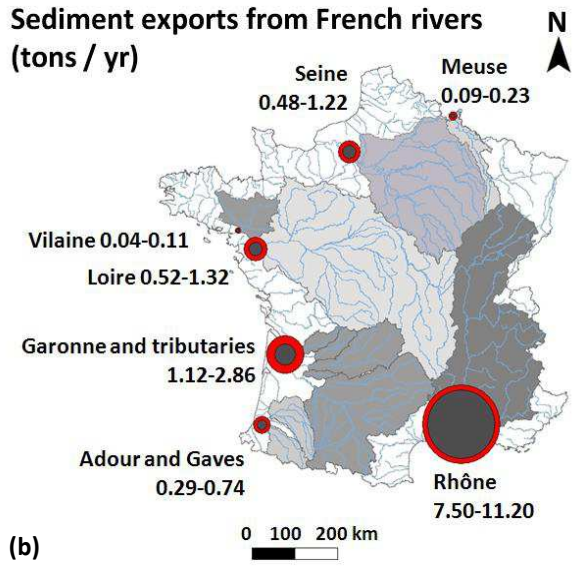

730
731
732
733